

# MiR-214-3p delays fracture healing in rats with osteoporotic fracture through inhibiting BMP/Smad signaling pathway

L.-G. ZHOU, P. SHI, Y.-J. SUN, H.-Z. LIU, J.-Q. NI, X. WANG

Department of Orthopaedics Traumatology, the Affiliated Yantai Yuhuangding Hospital of Qingdao University, Yantai, China.

Lugang Zhou and Peng Shi contributed equally to this work

**Abstract. – OBJECTIVE:** The purpose of this study was to explore the mechanism of micro-ribonucleic acid (miR)-214-3p in regulating fracture healing in rats with osteoporosis.

**MATERIALS AND METHODS:** A total of 30 female Sprague-Dawley rats were selected and randomly divided into 3 groups, including group A [phosphate-buffered saline (PBS), n=10], group B (AntagomiR-NC, n=10), and group C (AntagomiR-214-3p, n=10). All rats underwent ovariectomy, and the osteoporosis rat model was verified by dual-energy X-ray absorptiometry 8 weeks after the operation. Then the osteoporotic fracture was established in rats via a second operation. From the successful modeling until the 6<sup>th</sup> week, 50  $\mu$ L PBS (2 nmoL) was intraperitoneally injected in group A, an equal amount of AntagomiR-NC was injected in group B, and an equal amount of AntagomiR-214-3p was injected in group C once a week. At the 6<sup>th</sup> week, fracture healing of osteoporosis rats was evaluated. At the same time, the expression of miR-214-3p in the three groups was detected via reverse Transcription-Polymerase Chain Reaction (RT-PCR). Furthermore, the protein expressions of bone morphogenetic protein 2 (BMP2) and Smad4 in the three groups were detected via Western blotting (WB).

**RESULTS:** After ovariectomy, the bone mineral density in each group was significantly lower than that before ovariectomy, and the differences were statistically significant ( $p<0.05$ ). Imaging evaluation demonstrated that compared with group A and B, there were significantly more callus tissues in group C. Meanwhile, the fracture line healing was better and blurred, and the internal fixation had no displacement and loosening. RT-PCR results indicated that the expression level of miR-214-3p in group C was significantly lower than that of the other two groups ( $p<0.05$ ). WB results showed that the protein expression levels of BMP2 and Smad4 in group C were significantly higher than those of group A and group B ( $p<0.05$ ).

**CONCLUSIONS:** MiR-214-3p delays fracture healing in rats with osteoporotic fracture by inhibiting the BMP/Smad signaling pathway.

Key Words

MiR-214-3p, BMP/Smad signaling pathway, Osteoporotic fracture healing.

## Introduction

Osteoporosis is a common and frequently-occurring disease in the world, which can easily lead to low-energy and pernicious traumatic fracture. The low quality of bone in patients with an osteoporotic fracture may result in insufficient internal fixation strength and stability. Thus, the surgical intervention in these patients becomes very complicated. Clinically, osteoporosis is often diagnosed initially in the cases of fragility fracture<sup>1,2</sup>. Therefore, deeply understanding the possible underlying mechanism of osteoporosis in fracture healing is extremely important for reasonable clinical management of these patients.

Micro-ribonucleic acid (miRNA) is a kind of small-molecular non-coding RNA with about 19-25 nucleotides in length. MiRNA was first discovered by Lee et al<sup>3,4</sup> in *Caenorhabditis elegans*. It is reported that miRNA regulates gene expression at the post-transcriptional level by degrading its target messenger RNA (mRNA) or inhibiting mRNA translation. The near-perfect complementary pairing between miRNA and its target gene can lead to direct cleavage of target genes. However, the partial complementary pairing between them will result in the inhibition of target gene translation<sup>3,5-7</sup>. The final consequence of either mechanism is the decline in the protein expression levels of target genes. Currently, it is well known that miRNA plays an important role in various pathophysiological processes, including cell differentiation, cell cycle regulation and apoptosis<sup>8</sup>. Moreover, miRNA is known as a key regulatory factor for bone formation, bone

remodeling and the maintenance of bone homeostasis<sup>9,10</sup>. However, the studies on the function of miRNAs and their target genes remain limited.

At present, multiple studies have focused on exploring the abnormal expression of miRNAs in malignant tumors. Meanwhile, a large number of researches have demonstrated that miRNA is also involved in the pathophysiological processes of other diseases<sup>11-14</sup>. Some studies have manifested that miR-214-3p is highly expressed in osteoclasts in bone tissues of elderly females with osteoporosis. Furthermore, it can inhibit the activity of osteoblasts after being secreted out of cells, thereby reducing the osteogenic capability and delaying fracture healing<sup>15</sup>.

Bone morphogenetic proteins (BMPs) belong to the transforming growth factor- $\beta$  (TGF- $\beta$ ) superfamily, which plays important roles in bone development, bone growth after birth as well as fracture healing. As an important member of the BMP family, BMP2 participates in the early development and tissue construction of the skeletal system<sup>16</sup>. Meanwhile, some reports have indicated that BMP2 can induce osteoblast differentiation and increase bone matrix secreted by osteoblasts<sup>17</sup>. Smad4 is one of the members of the signal transducer protein Smad family. These members can be activated after the transmembrane serine-threonine receptors respond to the TGF- $\beta$  signal<sup>18,19</sup>. Smad4, as an intracellular transduction signal for TGF- $\beta$ , exerts important effects on the development and function of osteoblasts and osteoclasts in bone metabolism.

In this study, we first established an osteoporotic fracture rat model. In addition, we explored the potential mechanism of miR-214-3p and BMP/Smad signaling pathway in the fracture healing of rats with osteoporosis *in vivo*.

## Materials and Methods

### **Experimental Rats and Establishment of the Osteoporosis Rat Model**

This study was approved by the Animal Ethics Committee of Qingdao University Animal Center. A total of 30 female Sprague-Dawley (SD) rats (250-300 g) aged 12 weeks old were purchased from Shanghai Silaike Experimental Animal Co., Ltd. All rats were randomly divided into three groups, including group A [phosphate-buffered saline (PBS), n=10], group B (AntagomiR-NC, n=10) and group C (AntagomiR-214-3p, n=10). Before modeling, the bone mineral density (BMD) of rats

was measured by dual-energy X-ray absorptiometry (NORLAND Corporation, Cranbury, NJ, USA). All rats in the three groups received ovariectomy, and the osteoporosis rat model was successfully established. Before the operation, rats were first anesthetized with 3% pentobarbital sodium (30 mg/kg) (Sigma-Aldrich, St. Louis, MO, USA). Subsequently, the four limbs of rats were fixed, the hair was shaved off and the skin was incised. Then the ovary was removed through the retroperitoneal approach. After hemostasis *via* vascular ligation, the skin was sutured layer by layer. Next, 80 $\times$ 10<sup>4</sup> U penicillin (Shanghai Xianfeng Pharmaceutical Co., Ltd., Shanghai, China; batch No.: S100824) was intramuscularly injected in rats twice a day for 3 consecutive days. 8 weeks later, the BMD of rats was measured again using the dual-energy X-ray absorptiometry (NORLAND Corporation, Cranbury, NJ, USA). Finally, the successful establishment of the osteoporosis rat model was confirmed.

### **Establishment of the Osteoporosis Rat Model of Fracture and Treatment in Each Group**

After successful establishment of the osteoporosis rat model, all the 30 rats were anesthetized with 3% pentobarbital sodium (30 mg/kg) (Sigma-Aldrich, St. Louis, MO, USA). After that, the four limbs were fixed, and the left femur was exposed *via* surgical operation. Meanwhile, transverse fracture of the middle left femur was artificially made using the wire saw, followed by a reduction of the fracture and intramedullary fixation with 1.5 mm Kirschner wire. Finally, the incision was sutured. After the operation, 80 $\times$ 10<sup>4</sup> U penicillin (Shanghai Xianfeng Pharmaceutical Co., Ltd., Shanghai, China; batch No.: S100824) was intramuscularly injected in rats twice a day for 3 consecutive days. All rats were fed in separate cages with free access to the activity. The experimental environment was maintained at a constant temperature of 21°C under 12/12 h day-night cycle. From the successful modeling until the 6<sup>th</sup> week, 50  $\mu$ L PBS (2 nmoL) was intraperitoneally injected in group A, an equal amount of AntagomiR-NC was injected in group B, and an equal amount of AntagomiR-214-3p was injected in group C once a week.

### **Imaging Analysis**

After successful establishment of the osteoporotic fracture rat model and injection in the three groups, the fracture healing of all rats was observed *via* X-ray (50 kV, 50 mA, and 125 ms) at 7 d and 42 d, respectively. This included the analysis of internal fixation position, porosis and

fracture line healing. Each X-ray image was analyzed by a radiologist, a laboratory researcher and an orthopedist independently. After the final X-ray image analysis, the rats were decapitated. The callus tissues were removed from the corpse, placed in a cryogenic storage tube and quickly stored in liquid nitrogen for subsequent experiments. At the same time, the tube was stored in an ultra-low temperature artificial climate box.

#### **Reverse Transcription-Polymerase Chain Reaction (RT-PCR) Analysis**

After adding 2-3 mL TRIzol reagent (Invitrogen, Carlsbad, CA, USA), the callus tissues of the three groups were cut into pieces and fully ground into homogenized powder. Subsequently, they were transferred into 1.5 mL Eppendorf (EP) tubes and placed at room temperature for 5 min. After the samples were completely cleaved, total RNA of each sample was extracted according to the instructions of TRIzol method. Then, the absorbance ( $A_{260}/A_{280}$ ) ratio was determined to detect the concentration of extracted RNA. Finally, the stepwise amplification was performed according to the instructions, followed by RT-PCR analysis of the reaction product. Primer sequences for miR-214-3p were shown below: forward: 5'-GACAGCAGGCACAGACA-3'; reverse: 3'-GTGCAGGGTCCGAGG-5'.

#### **Western Blotting (WB) Analysis**

The callus tissues of the three groups were collected, washed twice with ice normal saline and ground evenly. According to the instructions of the whole protein extraction kit, lysis solution was added into the tissues and homogenized using a tissue homogenizer for 1 min, followed by centrifugation at 12000 g, 4°C for 10 min. The supernatant was collected, and the concentration of extracted protein was determined in strict accordance with the bicinchoninic acid protein concentration assay kit (BCA). The extracted protein samples were stored at -70°C for standby application. The extracted protein sample and 2 × loading buffer were mixed evenly at a volume ratio of 1:1, followed by a bath in boiling water for 5 min. After natural cooling, the mixture was stored in a 4°C refrigerator for standby application. Based on the molecular weight of the target proteins, the sodium dodecyl sulfate-polyacrylamide gel electrophoresis (SDS-PAGE) separation gel was prepared and solidified for about 1 h. Meanwhile, 5% SDS-PAGE spacer gel was prepared and solidified for about half an hour. The electrophoresis buffer was added and the denatured protein

samples were added into the loading well according to the protein concentration (the total protein content in each well should be the same). Then the samples were separated by electrophoresis at a constant voltage of 220 V until bromophenol blue reached the bottom of the gel. According to the molecular weight of target protein, the gel was cut and incubated with transfer buffer. A layer of polyvinylidene difluoride (PVDF) membrane (Millipore, Billerica, MA, USA) and 6 layers of filter paper were cut according to the size of the gel. PVDF membranes were first soaked in methanol for 10 s. Subsequently, the PVDF membranes and filter paper were put into the transfer buffer. The positive electrode, 3 layers of filter paper, PVDF membrane, gel, 3 layers of filter paper and the negative electrode were placed in the transfer apparatus in order. The edge should be aligned and the bubble should be avoided. After 2 h of membrane transfer at a constant voltage of 110 V, the protein-attached PVDF membranes were sealed in 5% skim milk powder at room temperature for 2 h on a shaking table. The membranes were washed with Tris-Buffered Saline with Tween-20 (TBST) for 5 min and incubated with the primary antibody at a corresponding ratio at 4°C overnight. After washing with TBST 3 times (10 min/time), the membranes were incubated with the corresponding secondary antibody at room temperature for 3 h on a shaking table. Then, the membranes were washed again with TBST 3 times (10 min/time). The gel imager was preheated for 30 min. Meanwhile, the reagent A and B in the enhanced chemiluminescence (ECL) kit (Thermo Fisher Scientific, Waltham, MA, USA) were mixed evenly at an equal volume and dropwise added onto the PVDF membrane, followed by color development in the dark for 1 min. Excess liquid around the membrane was sucked dry using the filter paper, and the membrane was placed in the gel imager. Next, the bands were observed under a dynamic integral mode. Finally, the image was analyzed using the image analysis software.

#### **Statistical Analysis**

Statistical Product and Service Solutions (SPSS) 21.0 software (IBM, Armonk, NY, USA) was used for the statistical analysis. All experimental data were expressed as mean ± standard error of mean (Mean ± SEM). The *t*-test was used to compare the differences between the two groups. ANOVA was used for comparing the differences among groups, followed by Post-Hoc Test (Least Significant Difference).  $p < 0.05$  was considered statistically significant.

**Table I.** Measurement results of BMD in the three groups of rats before and after ovariectomy.

Group	BMD before ovariectomy (g/cm <sup>2</sup> )	BMD at 8 weeks after ovariectomy (g/cm <sup>2</sup> )
Group A	0.3924±0.0042	0.2104±0.0036
Group B	0.3946±0.0039	0.2112±0.0043
Group C	0.3918±0.0048	0.2109±0.0038

## Results

### **Establishment of the Osteoporosis Rat Model**

After the 30 SD female rats were numbered, the BMD was measured by dual-energy X-ray absorptiometry (Table I). All the 30 SD rats were randomly divided into three groups, including group A (PBS, n=10), group B (AntagomiR-NC, n=10), and group C (AntagomiR-214-3p, n=10). All rats in the three groups received ovariectomy, and BMD was measured again using the dual-energy X-ray absorptiometry after 8 weeks (Table I). Results showed that the BMD of each group after ovariectomy was significantly lower than that before ovariectomy, and the differences were statistically significant ( $p < 0.05$ ). This indicated the successful establishment of the osteoporosis rat model.

### **Establishment of the Osteoporotic Fracture Rat Model**

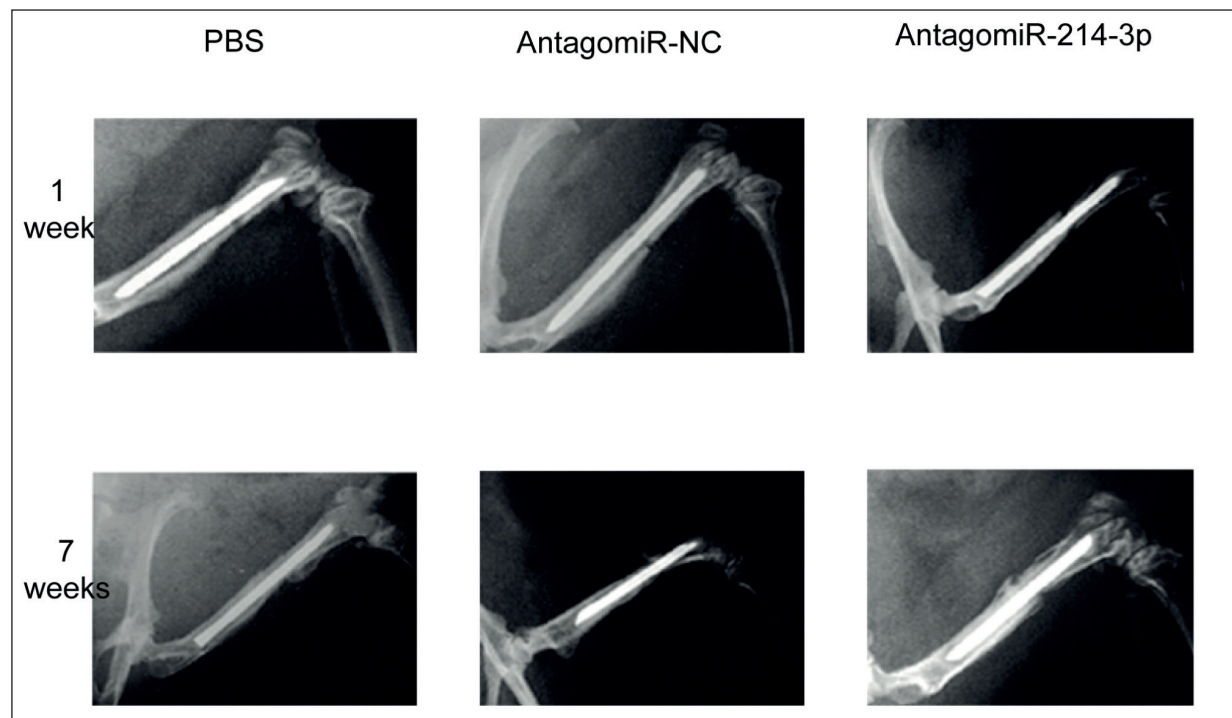
After the dual-energy X-ray absorptiometry was used to confirm the successful establishment of the osteoporosis rat model, the ovary was removed *via* operation. Subsequently, the osteoporotic fracture model was successfully established in rats.

### **Imaging Analysis**

Imaging evaluation demonstrated that compared with group A and B, there were more callus tissues in group C. Meanwhile, the fracture line healing was better and blurred, and the internal fixation had no displacement and loosening. These findings suggested that inhibiting the expression of miR-214-3p could promote fracture healing in rats with osteoporosis (Figure 1).

### **Expression of miR-214-3p in the Three Groups**

After successful establishment of the osteoporotic fracture rat model, 50  $\mu$ L PBS (2 nmol) was intraperitoneally injected in group A, an equal amount of AntagomiR-NC was injected in group B, and an equal amount of AntagomiR-214-3p was injected in group C once a week until the 6<sup>th</sup> week. Then the rats were decapitated, and the

**Figure 1.** Imaging evaluation at 1 week and 7 weeks after the operation.

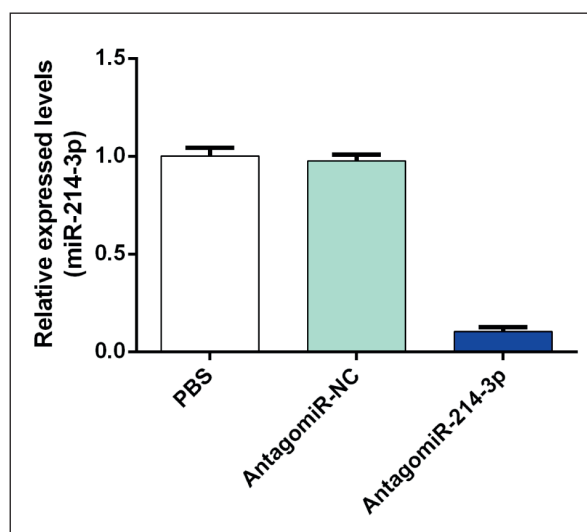


**Figure 2.** MiR-214-3p expression in the three groups was detected via RT-PCR. The expression of miR-214-3p in group C was significantly declined when compared with that of group A and group B ( $p < 0.01$ ).

expression of miR-214-3p in callus tissues of the three groups was detected *via* RT-PCR. Results revealed that there was no statistically significant difference in the expression of miR-214-3p between group A and group B ( $p > 0.05$ ). However, the expression level of miR-214-3p in group C was significantly lower than that of the other two groups, and the differences were statistically significant ( $p < 0.01$ ) (Figure 2).

#### **The Levels of BMP2 and Smad4 Elevated after miR-214-3p Downregulation**

Subsequently, the protein expression levels of BMP2 and Smad4 in callus tissues of the three groups were detected *via* WB. Results indicated that the protein expression of BMP2 in group C

was significantly increased when compared with that of the other two groups ( $p < 0.05$ ) (Figure 3A). As shown in Figure 3B, the protein expression of Smad4 in group C was also remarkably higher than that of the other two groups ( $p < 0.05$ ).

## **Discussion**

In recent years, there have been a large number of studies on the mechanism of osteoporotic fracture healing. Increasing evidence has suggested that miRNA plays an important role in the process of osteoporotic fracture healing<sup>20</sup>. Wang et al<sup>21</sup> have found that the expression level of miR-214 is associated with the decrease of bone formation in tissue samples of elderly patients, suggesting that miR-214 may play an important role in inhibiting bone formation. Li et al<sup>15</sup> have reported that the implantation of bone mesenchymal stem cells with inhibited expression of miR-214 into the rat model promotes osteoporotic fracture healing. However, implanting bone mesenchymal stem cells with BMP2 overexpression into the osteoporotic fracture rat model fails to promote fracture healing. The fracture healing is significantly accelerated after bone mesenchymal stem cells with miR-214 inhibition and BMP2 overexpression are implanted into the osteoporosis rat model. This indicates that there is a synergistic effect between the inhibition of miR-214 expression and the promotion of BMP2 expression<sup>22</sup>. Our findings were inconsistent with the above results. The expression level of miR-214-3p was inhibited in group C. Moreover, imaging evaluation showed that it could accelerate osteoporotic fracture healing in rats.

The Smad-dependent pathway is a classical BMP signal transduction pathway. It is known that the BMP/Smad signal transduction pathway

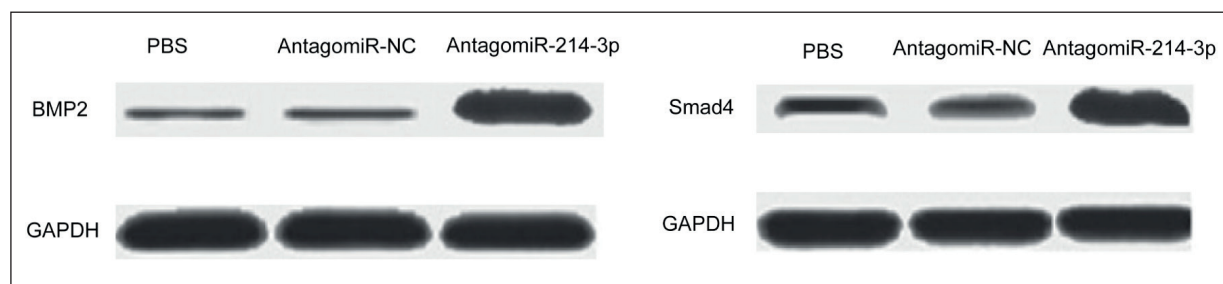


**Figure 3. A,** The protein expression of BMP2 in group C was significantly increased when compared with that of group A and group B ( $p < 0.05$ ). **B,** The protein expression of Smad4 in group C was remarkably increased when compared with that of group A and group B ( $p < 0.05$ ).

is composed of BMP signal, BMP receptor and receptor substrate Smad signal molecule<sup>23</sup>. The BMP ligand acts as a type II membrane receptor, which is activated by autophosphorylation. Subsequently, the type I membrane receptor is activated, thereby forming a heteromultimeric complex, phosphorylating Smad1, Smad5, and Smad8, as well as transmitting signals into cells<sup>24</sup>. Activated R-Smad and Smad4 can bind to the cytoplasm to form the R-Smad/Smad4 complex. This may ultimately transmit signals into the nucleus and bind to its target gene, and activate target gene transcription or complete signal transduction<sup>25</sup>. A large number of studies have demonstrated that TGF- $\beta$ /BMP signal plays an important role in regulating osteogenesis and bone formation<sup>26</sup>. In this work, results found that the expression of miR-214-3p was significantly inhibited in group C. WB results revealed that the protein expressions of BMP2 and Smad4 in group C were significantly increased when compared with those of the other two groups. Meanwhile, Li et al<sup>15</sup> have found that there is a synergistic effect between the inhibition of miR-214 expression and promotion of BMP2 expression in promoting osteoporotic fracture healing. Therefore, it is suggested that miR-214 may delay osteoporotic fracture healing by inhibiting the BMP/Smad signaling pathway.

In this study, we established an osteoporotic fracture rat model. 50  $\mu$ L PBS (2 nmol/L) was intraperitoneally injected in group A, an equal amount of AntagomiR-NC was injected in group B, and an equal amount of AntagomiR-214-3p was injected in group C. Imaging evaluation showed that compared with those in group A and B, there were more callus tissues found in group C. Meanwhile, the fracture line healing was better and blurred, and the internal fixation had no displacement and loosening. RT-PCR results demonstrated that the expression level of miR-214-3p in group C was significantly lower when compared with that of the other two groups. Moreover, WB results indicated that the protein expression levels of BMP2 and Smad4 in group C was significantly increased when compared with the other two groups. Inhibiting the expression of miR-214-3p in rats with osteoporotic fracture could activate the BMP/Smad signaling pathway, and promote osteoporotic fracture healing in rats. To sum up, our findings showed that miR-214-3p delayed fracture healing in rats with osteoporotic fracture by inhibiting the BMP/Smad signaling pathway. This experiment provides a living model for further study of the mechanism of osteoporotic fracture

healing, which also lays a solid foundation for an in-depth study on the osteoporotic fracture healing in human. However, more comprehensive studies are still needed for further exploring the mechanism of osteoporotic fracture healing.

## Conclusions

We showed that miR-214-3p delayed the fracture healing in rats with osteoporotic fracture by inhibiting the BMP/Smad signaling pathway. In addition, miR-214-3p could be used as an effective target molecular for the treatment of the fracture.

## Conflict of Interests

The authors declare that they have no conflict of interest.

## References

- 1) REBOLLEDO BJ, UNNANUNTANA A, LANE JM. A comprehensive approach to fragility fractures. *J Orthop Trauma* 2011; 25: 566-573.
- 2) GOLDBAHN J, LITTLE D, MITCHELL P, FAZZALARI NL, REID IR, ASPENBERG P, MARSH D. Evidence for anti-osteoporosis therapy in acute fracture situations--recommendations of a multidisciplinary workshop of the International Society for Fracture Repair. *Bone* 2010; 46: 267-271.
- 3) BARTEL DP. MicroRNAs: genomics, biogenesis, mechanism, and function. *Cell* 2004; 116: 281-297.
- 4) LEE RC, FEINBAUM RL, AMBROS V. The *C. elegans* heterochronic gene *lin-4* encodes small RNAs with antisense complementarity to *lin-14*. *Cell* 1993; 75: 843-854.
- 5) VALENCIA-SANCHEZ MA, LIU J, HANNON GJ, PARKER R. Control of translation and mRNA degradation by miRNAs and siRNAs. *Genes Dev* 2006; 20: 515-524.
- 6) WINTER J, JUNG S, KELLER S, GREGORY RI, DIEDERICH S. Many roads to maturity: microRNA biogenesis pathways and their regulation. *Nat Cell Biol* 2009; 11: 228-234.
- 7) HAMMOND SM, CAUDY AA, HANNON GJ. Post-transcriptional gene silencing by double-stranded RNA. *Nat Rev Genet* 2001; 2: 110-119.
- 8) HE L, HANNON GJ. MicroRNAs: small RNAs with a big role in gene regulation. *Nat Rev Genet* 2004; 5: 522-531.
- 9) LIAN JB, STEIN GS, VAN WIJNEN AJ, STEIN JL, HASSAN MO, GAUR T, ZHANG Y. MicroRNA control of bone formation and homeostasis. *Nat Rev Endocrinol* 2012; 8: 212-227.
- 10) TAIPALEENMAKI H, BJERRE HL, CHEN L, KAUPPINEN S, KASSEM M. Mechanisms in endocrinology: micro-RNAs: targets for enhancing osteoblast differentiation and bone formation. *Eur J Endocrinol* 2012; 166: 359-371.

- 11) LIU ZH, SUN XP, ZHOU SL, WANG HX. Research on the relations between the variation of miRNA-184 before and after treatment of acute myocardial infarction and prognosis. *Eur Rev Med Pharmacol Sci* 2017; 21: 843-847.
- 12) GAUDET AD, FONKEN LK, WATKINS LR, NELSON RJ, POPOVICH PG. MicroRNAs: roles in regulating neuroinflammation. *Neuroscientist* 2018; 24: 221-245.
- 13) GOLDBERGOVA MP, IPKOVA J, FEDORKO J, SEVCIKOVA J, PARENICA J, SPINAR J, MASARIK M, VASKU A. MicroRNAs in pathophysiology of acute myocardial infarction and cardiogenic shock. *Bratisl Lek Listy* 2018; 119: 341-347.
- 14) MALEMUD CJ. MicroRNAs and osteoarthritis. *Cells* 2018; 7: 92.
- 15) LI D, LIU J, GUO B, LIANG C, DANG L, LU C, HE X, CHEUNG HY, XU L, LU C, HE B, LIU B, SHAIKH AB, LI F, WANG L, YANG Z, AU DW, PENG S, ZHANG Z, ZHANG BT, PAN X, QIAN A, SHANG P, XIAO L, JIANG B, WONG CK, XU J, BIAN Z, LIANG Z, GUO DA, ZHU H, TAN W, LU A, ZHANG G. Osteoclast-derived exosomal miR-214-3p inhibits osteoblastic bone formation. *Nat Commun* 2016; 7: 10872.
- 16) ROSEN V. BMP2 signaling in bone development and repair. *Cytokine Growth Factor Rev* 2009; 20: 475-480.
- 17) CHATAKUN P, NUNEZ-TOLDRA R, DIAZ LE, GIL-RECIO C, MARTINEZ-SARRA E, HERNANDEZ-ALFARO F, FERRES-PADRO E, GINER-TARRIDA L, ATARI M. The effect of five proteins on stem cells used for osteoblast differentiation and proliferation: a current review of the literature. *Cell Mol Life Sci* 2014; 71: 113-142.
- 18) MATSUO SE, FIORE AP, SIGUEMATU SM, EBINA KN, FRIGUGLIETTI CU, FERRO MC, KULCSAR MA, KIMURA ET. Expression of SMAD proteins, TGF-beta/activin signaling mediators, in human thyroid tissues. *Arq Bras Endocrinol Metabol* 2010; 54: 406-412.
- 19) KIM BJ, HWANG JY, HAN BG, LEE JY, LEE JY, PARK EK, LEE SH, CHUNG YE, KIM GS, KIM SY, KOH JM. Association of SMAD2 polymorphisms with bone mineral density in postmenopausal Korean women. *Osteoporos Int* 2011; 22: 2273-2282.
- 20) NUGENT M. MicroRNAs and Fracture Healing. *Calcif Tissue Int* 2017; 101: 355-361.
- 21) WANG X, GUO B, LI Q, PENG J, YANG Z, WANG A, LI D, HOU Z, LV K, KAN G, CAO H, WU H, SONG J, PAN X, SUN Q, LING S, LI Y, ZHU M, ZHANG P, PENG S, XIE X, TANG T, HONG A, BIAN Z, BAI Y, LU A, LI Y, HE F, ZHANG G, LI Y. miR-214 targets ATF4 to inhibit bone formation. *Nat Med* 2013; 19: 93-100.
- 22) LI KC, CHANG YH, YEH CL, HU YC. Healing of osteoporotic bone defects by baculovirus-engineered bone marrow-derived MSCs expressing MicroRNA sponges. *Biomaterials* 2016; 74: 155-166.
- 23) EDLUND S, LANDSTROM M, HELDIN CH, ASPENSTROM P. Smad7 is required for TGF-beta-induced activation of the small GTPase Cdc42. *J Cell Sci* 2004; 117: 1835-1847.
- 24) KONSTANTINIDIS G, MOUSTAKAS A, STOURNARAS C. Regulation of myosin light chain function by BMP signaling controls actin cytoskeleton remodeling. *Cell Physiol Biochem* 2011; 28: 1031-1044.
- 25) JUN JH, YOON WJ, SEO SB, WOO KM, KIM GS, RYOO HM, BAEK JH. BMP2-activated Erk/MAP kinase stabilizes Runx2 by increasing p300 levels and histone acetyltransferase activity. *J Biol Chem* 2010; 285: 36410-36419.
- 26) RAHMAN MS, AKHTAR N, JAMIL HM, BANIK RS, ASADUZ-ZAMAN SM. TGF-beta/BMP signaling and other molecular events: regulation of osteoblastogenesis and bone formation. *Bone Res* 2015; 3: 15005.